ELSEVIER

Catalysis Today 70 (2001) 243–253

CATALYSIS TODAY

www.elsevier.com/locate/cattod

Computer modeling of the infrared spectra of zeolite catalysts

Konstantin S. Smirnov[a,b,*], Daniel Bougeard[b]

[a] Laboratory for Applied Organic Chemistry and Catalysis, Delft University of Technology,
Julianalaan 136, 2628 BL Delft, The Netherlands
[b] Laboratoire de Spectrochimie Infrarouge et Raman, UMR 8516 du CNRS Bât. C5, Université des Sciences et Technologies de Lille, 59655
Villeneuve d'Ascq Cedex, France

Abstract

The paper describes the applications of computer modeling methods to the interpretation of the infrared spectra of zeolite frameworks. The correlation of the breathing vibration of ring structures in zeolitic lattices with their infrared spectra was investigated by the molecular dynamics method. The calculations reveal that in periodic zeolite lattices the ring-breathing vibrations participate in many normal modes. Despite the fact that the ring-breathing vibrations are calculated to have characteristic frequencies, no general correlation of these frequencies with band positions in the infrared spectra was found.

Ab initio quantum-chemical calculations were employed to examine the band observed at 885 cm^{-1} in the infrared spectra of activated zeolite beta [J. Phys. Chem. B 104 (2000) 286]. In agreement with the assignment proposed from the experiments, the calculations show that the observed band belongs to a vibration of $-\mathrm{O}-\mathrm{Al(OH)}-\mathrm{O}-$ sites of the zeolite and ascribe this vibration to the antisymmetric stretching vibration of the O$-$Al$-$O bridge. © 2001 Elsevier Science B.V. All rights reserved.

Keywords: Infrared spectra; Zeolite catalyst; Computer modeling

1. Introduction

Zeolites are widely used in industry as gas separators, ion exchangers, and catalysts for fine chemicals. Vibrational spectroscopy of zeolitic systems provide a wealth of information about the dynamics of zeolite frameworks and the interaction of the guest species with catalytically active sites of the structures, and nowadays, spectroscopic measurements are widely employed in the studies of zeolitic materials. The application of vibrational spectroscopy necessitates reliable assignments of the observed features in the spectra. Unfortunately, due to the complexity of the zeolitic systems, such an assignment is not always considered straightforward solely on the basis of experimental data.

During the last decade, computer modeling has become an indispensable tool in zeolite studies. A variety of modeling methods based on either classical or quantum models have been used to elucidate the dynamics of zeolite lattices, the adsorption and diffusion of guest molecules, the isomorphic substitution of framework atoms, and to model the reactivity of the zeolite catalysts [1,2]. The capability of the computer modeling stems from the fact that the computational studies give detailed information about the behavior of the system at the microscopic level. Comparison of the modeling results with the experimental data permits the verification of the underlying model and, if the model appears to be valid, an interpretation of the experimental data is provided.

---

[*] Corresponding author. Present address: Laboratoire de Spectrochimie Infrarouge et Raman, UMR 8516 du CNRS Bât. C5, Université des Sciences et Technologies de Lille, 59655 Villeneuve d'Ascq Cedex, France. Fax: +33-3-204-36755.
E-mail address: konstantin.smirnov@univ-lille1.fr (K.S. Smirnov).

PII: S0920-5861(01)00421-7

The present paper exemplifies the application of different computer modeling techniques to the interpretation of the vibrational spectra of zeolite catalysts in terms of structural entities. The first part of the paper is devoted to a molecular dynamics study of pore-opening vibrations of ring structures in periodic zeolite frameworks. These vibrations have been the subject of many experimental and computational studies motivated by the wish to determine the regular structural units in the periodic lattices on the basis of their vibrational spectra.

The second part of the paper addresses the assignment of fingerprint bands in the infrared spectra of zeolite lattices. These bands are often attributed to vibrations localized on the defects of the frameworks. Specifically, ab initio quantum-chemical calculations of clusters representing a defect are used to determine the origin of such a band in the spectra of activated zeolite beta. The corresponding experimental infrared study of this catalyst has recently been reported by Vimont et al. [3].

2. Pore-opening vibrations of ring structures in zeolites

In 1971, Flaningen et al. [4,23] reported an extensive infrared study of zeolite structures and proposed a scheme for the assignment of bands in the IR spectra of zeolite frameworks. The authors suggested that the spectra of the lattices can be accounted for by assigning the observed bands to vibrations of primary (TO_4 tetrahedra, $T = Si, Al$) and secondary (combination of the tetrahedra) building units. Structure insensitive bands have been attributed to the intra-tetrahedral vibrations, while the bands showing a dependence on the framework topology were ascribed to vibrations of larger structural units such as rings, double rings, etc. Since that time, the scheme was widely applied in spectroscopic studies of zeolites and much attention was paid to identify the rings of different sizes from the observed IR spectra of zeolite lattices. Throughout the paper, the ring structures in zeolite frameworks will be denoted as *N*R, where *N* stands for the number of T (or O atoms) in the ring.

A number of modeling studies questioned the Flaningen's scheme [5–9]. Thus, Bornhauser and Calzaferri [7] studied the vibrational spectra of the molecular models of general formula $(HSiO_{3/2})_{2n}$, $n = 2, 3, 4, \ldots$ and reported that the pore-opening vibrations of ring structures occur in the 490–390, 440–250, and 340–210 cm^{-1} spectral regions for four-, five-, and six-membered rings, respectively. The authors found that for all the structures studied, the 4R pore-opening Raman active mode appears in the interval 420–455 cm^{-1}. Iyer and Singer [8,9] investigated local modes in sodalite and zeolite A frameworks and found that some of the vibrations can be represented as linear combinations of modes localized on the 4R and 6R structures and within a narrow frequency interval. They found a high degree of transferability between the local modes of 4R rings in sodalite and zeolite A frameworks. In a recent study of the vibrations of isolated silica rings with the PM3 method, Sitarz et al. [10] concluded that the rings of different sizes indeed have characteristic "ring frequencies". These data seem to support the validity of the Flaningen's scheme. On the other hand, de Man and van Santen [5] performed a normal mode analysis of cluster and periodic zeolite models and concluded that there is no correlation between particular features in the spectra and the presence of large structural fragments in the zeolite frameworks. In a more recent study, the authors showed that no specific band can be assigned to a three-ring mode in the vibrational spectra of three-ring containing zeolitic silica polymorphs [6].

The scheme suggested in Refs. [4,23] is based on a tacit assumption that the normal modes of a periodic zeolite lattice can be described as the basis of normal modes of *isolated* secondary building units and that the frequencies of these *characteristic* vibrations do not significantly vary with the change of the framework topology. In other words, a localized vibration of a specific structural unit is a linear combination of a small number of normal modes, desirably one mode, of the lattice. Similarly, to the group frequency approach widely employed in the interpretation of the vibrational spectra of organic molecules, one could then use the infrared spectroscopy to identify the secondary structural units in the zeolitic frameworks.

The present section reports the results of a molecular dynamics study of pore-opening vibrations of rings of different sizes in zeolite lattices, namely sodalite (SOD), zeolite A (LTA), and faujasite (FAU). All these frameworks have four- and six-membered aluminosilicate rings as secondary structural units

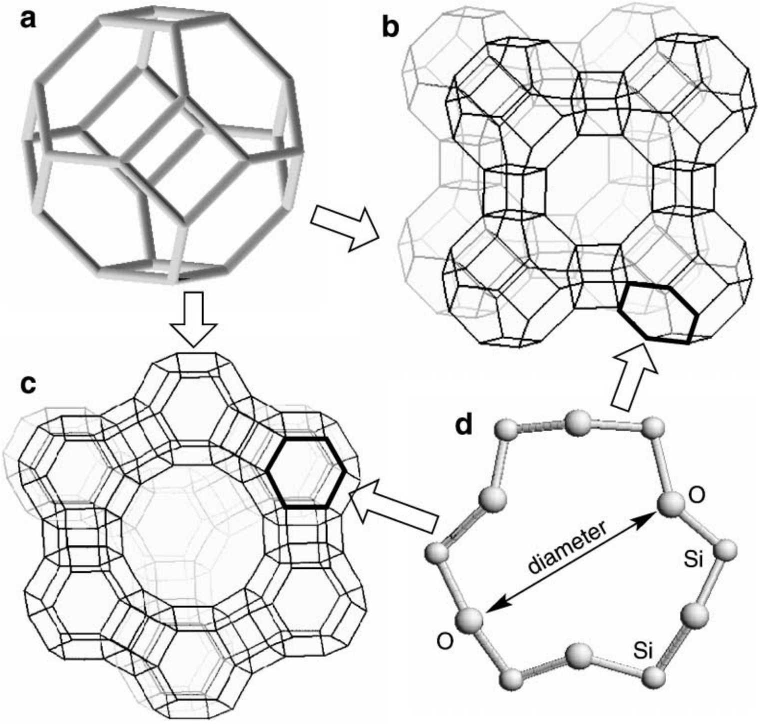

Fig. 1. Sodalite block (SOD) (a); frameworks of LTA (b) and FAU (c); zeolites formed by a combination of the blocks, and a presentation of a six-membered ring common to the structures (d).

which form a truncated cuboctahedron, the sodalite cage (Fig. 1a). The latter are then connected to each other in such a way that the complexity of the frameworks increases from SOD to FAU (Fig. 1b and c). Thus, in FAU framework, two types of 4R and 6R units can be distinguished. They are situated in sodalite blocks (4R-SOD, 6R-SOD) and in double 6R units (4R-D6R, 6R-D6R). LTA and FAU structures also possess rings of larger sizes, 8R and 12R, respectively, which form windows between the large cavities in the structures and control the diffusion of the adsorbed guest species. The study aims to analyze the relation between the pore-opening vibrations of the rings common to structures of different topologies and the vibrations and infrared spectra of the frameworks.

2.1. Calculations

The molecular dynamics calculations were carried out for pure siliceous zeolite structures with the use of a generalized valence force field potential model. The force field is a second-order Taylor expansion of the potential energy U with respect to internal coordinates (bond length, valence angles, etc.) and has the form

$$2U = \sum_{i,j} K_{ij}(s_i - s_i^0)(s_j - s_j^0), \qquad (1)$$

where s_i and s_i^0 are the instantaneous and equilibrium values of the internal coordinate i, respectively, and K_{ij} is the corresponding force constant. The force constants used in the simulations were taken from Ref. [11], where they were derived on the basis of ab initio calculations. This parameterization was shown to reproduce the zeolite IR and Raman spectra with a high degree of accuracy. The structural parameters for the zeolite frameworks and simulation conditions used in the calculations were described elsewhere [11,12] in detail.

The rings studied include 4R and 6R structures in all the frameworks. For a ring of size N, a pore-opening time-dependent vibrational coordinate $\mathcal{P}(t)$ can be defined as

$$\mathcal{P}(t) = \frac{1}{N/2} \sum_{i=1}^{N/2} R_i(t), \tag{2}$$

where $R_i(t) = D_i(t) - \bar{D}_i$, and $D_i(t)$ and $\bar{D}_i$ are the instantaneous and mean values of the ith diameter of the ring. The ring diameter is defined as the distance between oxygen atoms on the opposite sides of the ring (Fig. 1d). The $\mathcal{P}(t)$ coordinate is totally symmetric and corresponds to the breathing vibration of an isolated ring. The Fourier transform of the auto-correlation function of the $\mathcal{P}(t)$ coordinate yields the power spectrum of the ring-breathing vibration and contains all the involved frequencies. Operationally, it was found that the present definition leads to the same power spectra as the definition of the pore-opening via the area of the ring that was used by Schrimpf et al. [13].

It is important to notice that the coordinate defined by Eq. (2) describes the totally symmetric motion only and there also exist other pore-fluctuation coordinates. Thus, assuming at least a C_3 symmetry, two other coordinates describing elliptical distorsions of the ring can be formed for an isolated 6R ring:

$$\mathcal{E}_1(t) = 2R_1(t) - R_2(t) - R_3(t)$$
$$\text{and} \quad \mathcal{E}_2(t) = R_2(t) - R_3(t). \tag{3}$$

Note that these coordinates correspond to the degenerate frequencies. As before, the power spectrum of the coordinates can be obtained via the Fourier transformation of the corresponding auto-correlation function.

Infrared spectra of the zeolite frameworks were computed via the Fourier transformation of the dipole moment auto-correlation function using a procedure described elsewhere [12]. The frequency step in the calculated spectra is equal to 3.26 cm^{-1}.

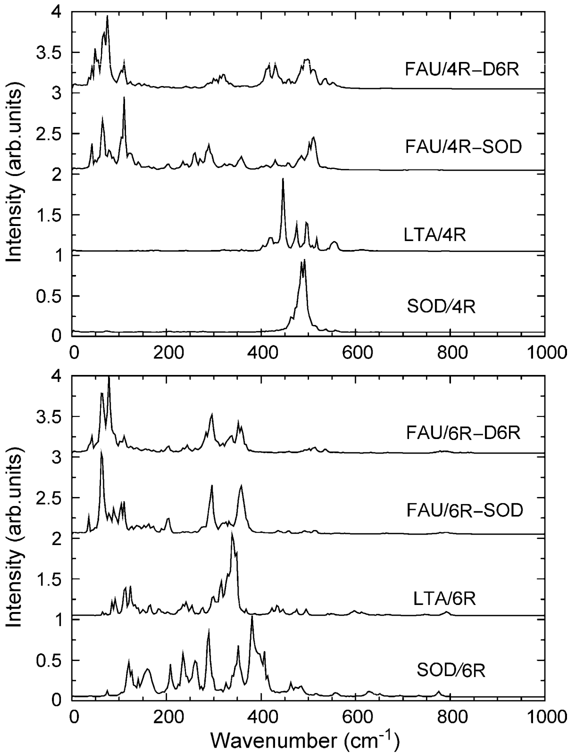

Fig. 2. Calculated power spectra of the pore-opening vibration of 4R rings (upper panel) and of 6R rings (lower panel) in the zeolite structures. See text for the abbreviations used.

2.2. Results and discussion

Fig. 2 shows the calculated power spectra of the pore-opening vibration in 4R and 6R structural units of the frameworks. In the SOD lattice, the vibration of the 4R ring has a simple spectrum and the figure shows that the pore-opening participates in normal modes within a narrow 100 cm^{-1} frequency interval. In the LTA lattice, the 4R pore-opening consists of normal modes in a twice as large frequency range as for the SOD framework. For the breathing 4R ring vibration in the FAU structure, the calculations reveal similar spectra for both the types of rings and indicate that the vibration is spread over many normal modes in a 500 cm^{-1} range. The increasing complexity of the spectrum reflects the increasing complexity in the zeolite topology. Fig. 2 demonstrates that the pore-opening vibration of the 6R structures has a more complex spectrum and that, like for the 4R units, the vibration in the FAU lattice has similar spectra for both the types of rings. Fig. 2 shows that for all frameworks, regardless of their complexity, the 6R pore-opening vibrations participate in many normal modes with frequencies spread over a wide interval.

The spectra presented in Fig. 2 show that the increase of the ring size leads to a decrease of the high-frequency limit of the ring-opening vibration. Thus, for 4R, the calculated limit has a value of ca. 550 cm^{-1} (LTA), whereas for 6R rings, the edge frequency is of ca. 420 cm^{-1} (SOD). This result is in line with the data of Bornhauser and Calzaferri [7] who calculated the pore-opening vibrations of the ring structures in the 490–390, 440–250, and 340–210 cm^{-1} spectral regions for four-, five-, and six-membered rings, respectively. Our study yields a broader frequency interval for the pore-opening vibration. This difference can be due to the use of a periodic model in the present study, while molecular models were employed in Ref. [7].

To extract a correlation between the spectra of the pore-opening vibrations in the frameworks, we formed a correlation spectrum as the product of the normalized spectra of a particular ring in all the frameworks. The correlation spectra are displayed in Fig. 3, which show that the 4R pore-opening vibration has a characteristic frequency in the interval of 480–510 cm^{-1}, whereas the 6R pore-opening motion appears in two narrow frequency intervals common to all the frameworks: 280–300 and 330–360 cm^{-1}. These characteristic frequency ranges are mostly well apart from the maxima of the bands calculated for each of the zeolites. The characteristic 4R opening frequency is in line with the values obtained in previous computational studies; 471 cm^{-1} [14], 455–451 cm^{-1} [15], and 448 cm^{-1} [8].

Fig. 4 presents the calculated infrared spectra of the lattices. Comparison of Figs. 3 and 4 indicates that no IR active modes in the spectra of SOD and LTA lattices can be ascribed to the 4R pore-opening vibration, whereas an intense IR band at 499 cm^{-1} in the infrared spectrum of FAU lattice correlates well with the 4R pore-opening. Nevertheless, it is also well known that all aluminosilicates have infrared bands in the region 450–520 cm^{-1} and thus no band in this frequency range can unambiguously pin-point the presence of the four-membered rings in the structure. A manifestation of the 6R opening-vibration can only be followed as very weak IR bands at 340 and 350 cm^{-1} for LTA and FAU frameworks, respectively, but no IR active mode can be attributed to the 6R vibration in SOD lattice.

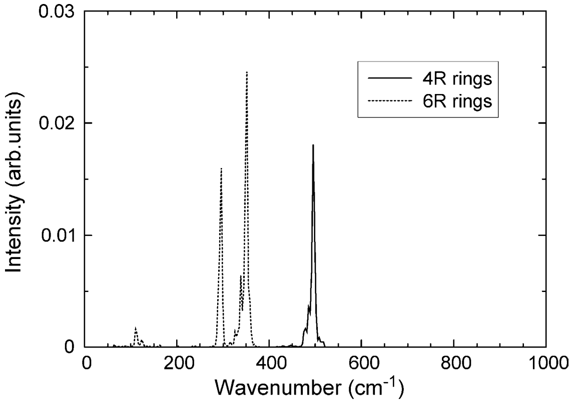

Fig. 3. Correlation spectra of 4R (solid line) and 6R (dotted line) pore-opening vibrations of the zeolite frameworks.

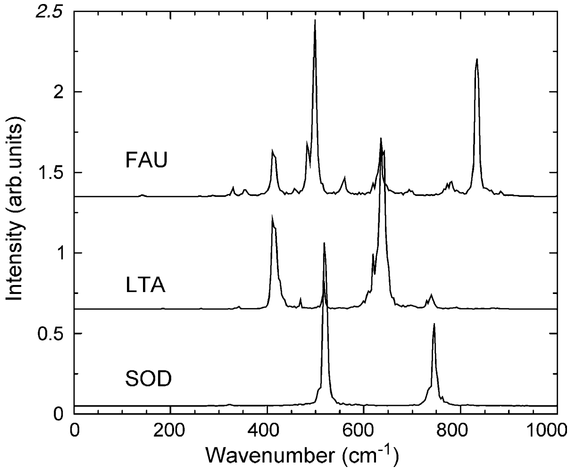

Fig. 4. Calculated infrared spectra of the zeolite frameworks. The spectra were cut at 1000 cm^{-1}.

As the infrared activity of the totally symmetric ring-breathing vibration comes from the variation of the dipole perpendicular to the ring plane, the vibration is expected to be only weakly IR active. Therefore, one might suppose that other ring vibrations such as those defined by Eq. (3) can be more characteristic for the IR spectra. Fig. 5 presents the power spectra of the $\mathcal{E}_1(t)$ and $\mathcal{E}_2(t)$ coordinates (Eq. (3)) for 6R units in the LTA framework. The figure shows that the spectra are almost identical to each other that reveals the degeneracy of the coordinates. Further, one can see that the frequencies involved in the elliptical distortions of the rings are mostly within interval 50–200 cm^{-1}, below the high-frequency limit of ring-breathing vibration (cf. Fig. 2). Despite these asymmetric ring vibrations are expected to be infrared active; comparison of Figs. 4 and 5 show no IR bands due to the vibrations.

The results presented above give rise to the question whether the normal modes of the smaller structural

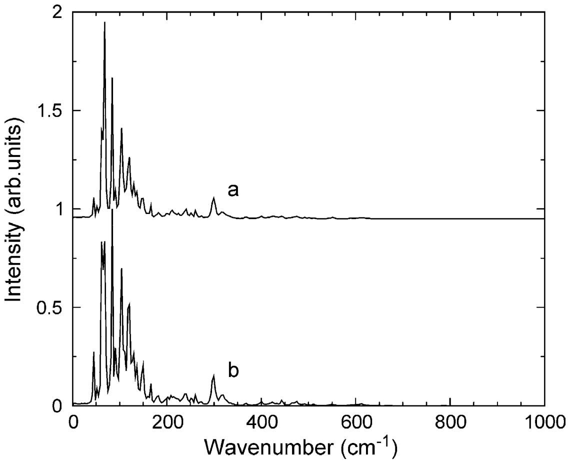

Fig. 5. Power spectra of the $\mathcal{E}_1(t)$ (a) and $\mathcal{E}_2(t)$ (b) coordinates defined by Eq. (3) for 6R rings of the LTA framework.

units can be used as a basis for the normal modes of the frameworks. Fig. 6 shows the spectra of the symmetric and antisymmetric combinations of the T–O stretching motions in T–O–T linkages, and the deformation of the T–O–T angles in the LTA structure. Strictly speaking, these combinations are not the normal coordinates of an isolated T–O–T bridge, but nevertheless, the figure clearly shows that only the antisymmetric combination participates in framework normal modes within a narrow frequency interval, whereas the other coordinates contribute to many modes over a wide spectral range. Therefore, the assignment of the observed bands to T–O–T bending, symmetric T–O stretching vibrations seems to be doubtful although the most significant contribution of these vibrations to framework modes occurs in specific frequency intervals, namely 700–800 and 50–200 cm^{-1} for the symmetric T–O stretching and T–O–T angle bending coordinates, respectively. On the contrary, the bands observed in the region 1000–1200 cm^{-1} can indeed be assigned to the antisymmetric T–O stretching vibration.

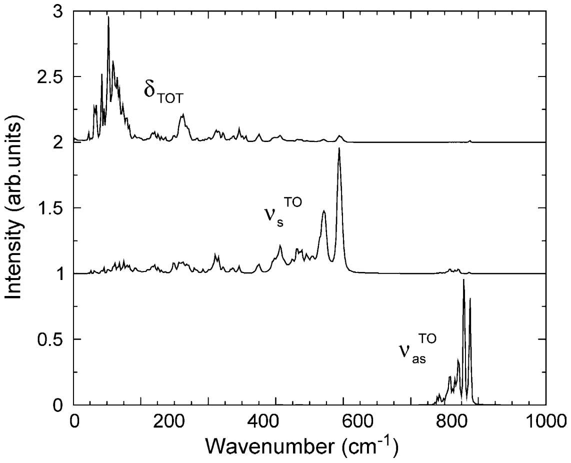

Fig. 6. Power spectra of antisymmetric (ν_{as}^{TO}) and symmetric (ν_s^{TO}) stretching T–O coordinates, and TOT angle bending coordinate (δ_{TOT}) of T–O–T linkages in the LTA structure.

The presented results therefore point to the absence of a general correlation between the pore-opening vibration of the ring structures with the infrared spectra of the zeolite frameworks. This result is in agreement with data of de Man and van Santen [5]. The study also indicates that the normal modes of zeolite lattices can hardly be represented via normal modes of structural units forming the zeolite lattice, especially if large building blocks are involved.

3. Localized vibrations of zeolitic frameworks

The previous section reveals the absence of infrared bands specific to the vibrations of structural subunits in the regular periodic frameworks. Nevertheless, fingerprint bands are sometimes observed in the IR spectra and the bands are often attributed to vibrations localized on the defects of a zeolite lattice. Thus, isomorphously substituted Ti zeolite structures show a distinct peak at approximately 960 cm^{-1} and the presence of this peak is generally considered as an evidence for the incorporation of the Ti atoms into the lattices [16]. Modeling studies of Ti-substituted structures showed that the band at 960 cm^{-1} is due to a vibration localized in Si–O–Ti bridges of the zeolitic frameworks [17,18] but slightly differs in the attribution of the vibration. While in Ref. [17] the band was assigned as the antisymmetric vibration of the Si–O–Ti bridges, the authors of Ref. [18] claimed that it is mostly due to the vibration of the Si–O bond in the bridges. A recent MD study [19] has confirmed the validity of the assignment proposed by de Man and Sauer [17]. Both the quantum-chemical calculations [17] and classical MD simulations [18,19] showed that the localization is due to the difference between the force constants of the Si–O and Ti–O bonds, whereas the difference in masses of the Si and Ti atoms cannot explain the frequency of the band.

Very recently, Lavalley and co-workers [3] observed a fingerprint band, which appeared at 885 cm^{-1} in the IR spectra after activation of zeolite beta. The band was shown as belonging to the strong Lewis acid sites and it was attributed to a vibration in a moiety consisting of a monohydroxylated trivalent aluminum atom partly bound to the framework (–O–Al(OH)–O–). This part of the paper reports ab initio quantum-chemical calculations of molecular models that mimic the site proposed by Lavalley and co-workers [3]. The aim of the study was to find out whether the proposed structure leads to the calculated characteristic frequencies compatible with the experimental IR data.

3.1. Calculations

The studied molecular models H_3Si–O–Al(OH)–O–SiH_3 (I), F_3Si–O–Al(OH)–O–SiF_3 (II), and $(OH)_3Si$–O–Al(OH)–O–$Si(OH)_3$ (III) are shown in Fig. 7. In order to estimate the influence of the terminating atoms on the results of the calculations, the terminating hydrogens of model I were substituted by the fluorine atoms in model II and hydroxyl groups in model III. In addition, terminating the cluster by fluorine atoms, which are isoelectronic to OH groups, avoids the formation of intramolecular hydrogen bonds that can bias the results of the calculations. The increasing size of the models should also permit us to assess the transferability of the results to the periodic zeolite frameworks. The central part of the molecular models represents the –O–Al(OH)–O– active site proposed by Lavalley and co-workers [3] as the origin of the observed fingerprint band in the IR spectra of activated zeolite beta.

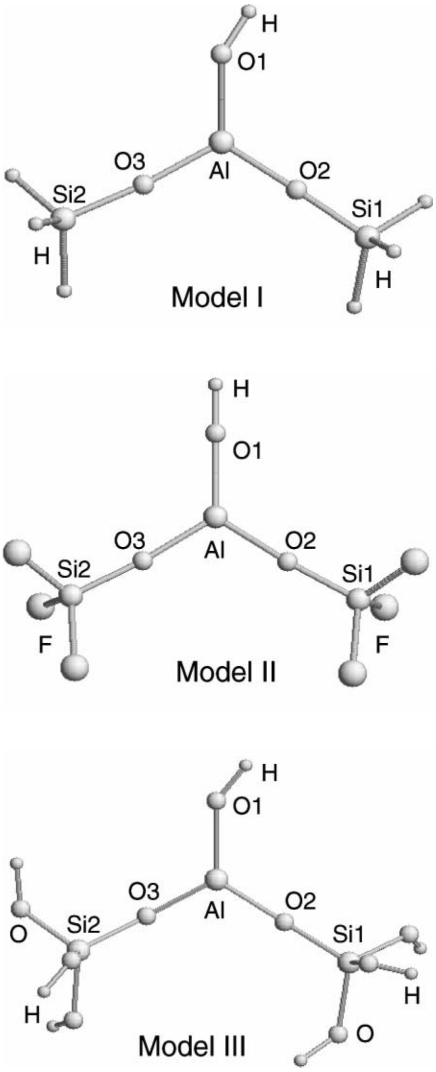

Fig. 7. Optimized structures of the molecular models used in the ab initio calculations. The numbering of atoms corresponds to the numbering used in Table 1.

In contrast to the first part of the paper, the calculations of the second part were carried out using a method of quantum chemistry. A deficiency of the classical methods stems from the use of a force field model, which is typically parameterized for a specific bonding situation. For example, the force field employed in the first part was derived for *regular* TO_4 tetrahedra. Thus, the use of a classical method for a study of defect sites, like in the present case, would necessitate the use of an environment-dependent force field model. This is unavailable for the system of interest. Further, the structure of the defect, which is different from the regular TO_4 tetrahedra of a zeolite lattice, indicates that the corresponding vibrations could be localized modes and therefore a cluster approach could be sufficient to treat the problem. These considerations have determined the choice of the method and models employed in the second part of the paper.

The calculations were performed using the GAMESS package [21] with the 3-21G* basis set at the Hartree–Fock (HF) level. This basis set provides a good compromise between the reliability of the results and the computational time and it was successfully employed in the development of the ab initio force field for aluminosilicate structures [11,20]. Since quantum-chemical calculations overestimate the strength of the chemical bonds and consequently the vibrational frequencies, a scaling factor of 0.9 was applied to the computed frequencies. This value of the scaling factor was obtained in Refs. [11,20] for aluminosilicate clusters computed with the 3-21G* basis set and the precision achieved for the vibrational spectra of several zeolitic frameworks with this scaling factor and basis set was sufficiently high. The geometry of the molecules was optimized in the C_1 space group without any constraint and a vibrational analysis in the harmonic approximation was then carried out to obtain the normal modes of the models. No correction for anharmonicity of the vibrations was made since for normal modes involving displacements of heavy atoms the anharmonicity does not play an important role.

3.2. Results and discussion

Table 1 lists the optimized values of the internal coordinates in the –Si–O–Al(OH)–O–Si– moiety in the models and their optimized structures are shown in Fig. 7. The three-fold coordination of the Al atom leads to relatively short Al–O bonds (by ca. 0.04–0.06 Å) as compared to the bonds for the atoms in four-fold coordination [20,22]. Such a bonding situation also results in almost linear Si–O–Al angles in all the models. The substitution of the terminating hydrogens in the model I by the fluorine atoms in the model II causes noticeable changes in the optimized values of the internal coordinates. Thus, model II has an almost linear Al–O1–H angle, while in models I and III the optimized values are 146.7° and 141.14°, respectively. Further, the substitution causes a shortening of the Al–O1 and Si–O bonds, by ca. 0.02–0.03Å, and a slight decrease of the O1–H bond length. In contrast, the Al–O2 and Al–O3 bonds are slightly longer in model II. For all the three models, the O–Al–O angles are calculated in the range 117–122° indicating a planar structure of the AlO_3 unit.

Table 1
Optimized values of the internal coordinates of the –Si–O–Al(OH)–O–Si– moiety in the models. Bond lengths and bond angles are in Å and degrees, respectively. The numbering of atoms corresponds to that in Fig. 7

Internal coordinate	Model I	Model II	Model III
O1–H	0.951	0.947	0.953
O1–Al	1.655	1.627	1.662
O2–Al	1.674	1.679	1.670
O3–Al	1.670	1.679	1.670
O2–Si1	1.628	1.585	1.610
O3–Si2	1.628	1.585	1.609
Al–O1–H	146.70	179.49	141.14
Al–O2–Si1	177.60	175.62	171.62
Al–O3–Si3	175.40	176.81	167.18

Discussing the results of the vibrational analysis, we concentrate on the spectral region 800–1000 cm^{-1}, where the experimental fingerprint band appears. In addition, we choose modes involving large displacements of atoms in the –Si–O–Al(OH)–O–Si– moiety of the models. It is noteworthy that such a separation is not always straightforward because, generally, a normal mode includes the displacements of all the atoms.

Table 2 gathers the calculated vibrational frequencies of the models in the frequency region of interest. The table shows that the model I exhibits only one mode in contrast to three modes in models II and III. Comparison of the internal coordinates involved in the modes shows that the single mode at 919 cm^{-1} of the model I matches well the modes at 981 and 935 cm^{-1} of models II and III, respectively. The other modes of model I comparable to the modes of models II and III reported in Table 2 have frequencies at 629 and 1133 cm^{-1}, outside of the frequency range of interest, the modes involve the antisymmetric stretching vibration of the O2–Al–O3 bridge. The former mode also includes a vibration of the SiH_3 groups as rigid units explaining its low frequency, and the latter involves the angle-bending coordinates of $OSiH_3$ groups. This frequency difference between model I and models II and III is due to the use of the light hydrogens as the terminating atoms in the model I.

Despite the difference in the optimized geometries of models II and III, the computed vibrational modes of these models reveal a good transferability (Table 2). Both the vibrational frequencies and the internal coordinates involved in the modes are in good agreement for both the models. While going from

Table 2
Calculated vibrational frequencies (in cm^{-1}) of the models in the frequency region 800–1000 cm^{-1}. The scaled frequencies are reported

Model	Frequencies[a]	Assignment[b]
H_3Si–O–Al(OH)–O–SiH_3	919 (898)	ν(Al–OH) + δ(AlOSi) + ω($OSiH_3$)
F_3Si–O–Al(OH)–O–SiF_3	857 (854) 898 (898) 981 (967)	ν_s(AlO_3) + ω($OSiF_3$) ν_{as}(O–Al–O) + ω($OSiF_3$) ν(Al–OH) + δ(AlOSi) + ν(Si–O)
$(OH)_3Si$–O–Al(OH)–O–$Si(OH)_3$	840 (834) 883 (883) 935 (919)	ν_s(AlO_3) + ω($OSi(OH)_3$) ν_{as}(O–Al–O) + ω($OSi(OH)_3$) ν(Al–OH) + δ(OAlO) + ω($OSi(OH)_3$)

[a] Values given in parentheses correspond to the frequencies computed for –O–Al(OD)–O– models.

[b] ν and δ denote the bond stretching and angle-bending vibrations, respectively. ω stands for a complex vibration involving several internal coordinates.

model II to model III, a systematic downward shift of the vibrational frequencies is computed. Besides the different optimized structures, this shift can be due to the increase in the number of degrees of freedom in model III. The transferability is further supported by the frequency shift computed on the substitution of the hydrogen atom in the O1H group by deuterium (Table 2).

Among the modes calculated in the frequency region of interest, the modes with frequencies of 898 and 883 cm^{-1} for the models II and III, respectively, seem to be the best candidates to account for the band observed in the spectra of the activated zeolite beta. The calculated frequencies of the mode are in perfect agreement with the band observed at 885 cm^{-1}. However, this nice coincidence should be regarded with caution because of the approximative character of the used scaling factor. Nevertheless, further support for the assignment comes from the fact that the frequencies of the modes do not change upon the isotopic substitution (Table 2) in agreement with the experimental results [3]. The atomic displacements in the mode for

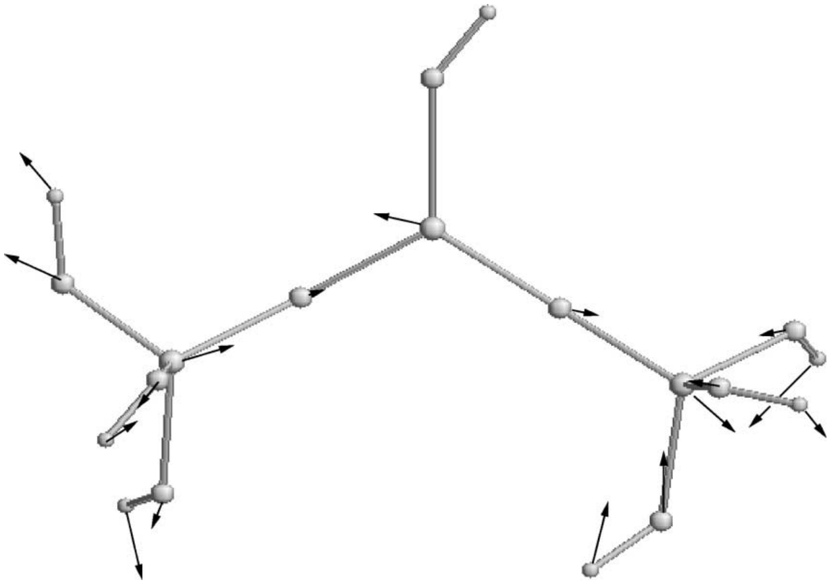

Fig. 8. Displacements of atoms of the model III in the vibrational mode with a frequency of 883 cm^{-1}.

the model III are shown in Fig. 8. One sees that this vibration does not involve displacements of atoms in the O1H group; this explains its insensitivity to the isotopic exchange. On the other hand, since such a structural unit is a strong Lewis site, the adsorption of basic molecules such as pyridine, occurring via donation of the lone-electron pair to accepting orbitals of the Al atom, will strongly affect the vibrational mode. This was indeed observed in the experiment [3].

The results of the calculations allow us to conclude that the band at 885 cm^{-1} in the IR spectra of the activated zeolite beta is indeed due to the vibration of –O–Al(OH)–O– moiety, as it was suggested by Lavalley and co-workers [3]. According to the calculations, this vibration can be described as the antisymmetric stretching vibration of O–Al–O bridge.

Taking into account the above data and recalling the results of Refs. [17–19], one might conclude that the fingerprint bands in the spectra of zeolitic frameworks are due to the *antisymmetric* vibrations of specific structures. This conclusion correlates with the results of the first part of the paper where it was shown that the antisymmetric vibrations of the O–T–O units can be, in a good approximation, used as a basis for the normal modes of the frameworks.

4. Conclusions

Computer modeling techniques were used to investigate the infrared spectra of the zeolite catalysts. The molecular dynamics method was employed to look for a correlation between the pore-opening vibration of rings in zeolitic lattices and the infrared spectra of the frameworks. The results of the calculations show that the breathing vibration of four- and six-membered rings is involved in many normal modes of zeolitic lattices. The pore-opening vibrations were calculated in the 480–510 cm^{-1} frequency range for 4R rings, and 280–300 and 330–360 cm^{-1} intervals for 6R rings. However, no general correlation of the pore-opening motions with the infrared spectra of the frameworks was found.

The origin of the fingerprint band at 885 cm^{-1} observed in the infrared spectra of activated zeolite beta was studied by ab initio quantum-chemical calculations of molecular models, which mimic the structure suggested on the basis of experimental data [3]. In fair agreement with the assignment deduced from the spectroscopic measurements, the results of the calculations show that the band is due to the antisymmetric stretching vibration of O–Al–O bridge in –O–Al(OH)–O– site in the zeolite.

The two particular examples presented clearly demonstrate the capability of computer modeling as a valuable tool for the interpretation of data of spectroscopic measurements.

Acknowledgements

KSS thanks Delft University of Technology for the research fellowship. The allocation of computer time at Centre of High Performance Applied Computing of Delft University of Technology is gratefully acknowledged.

References

[1] C.R.A. Catlow (Ed.), Computer Modeling of Structure and Reactivity of Zeolites, Academic Press, London, 1992.
[2] B. van de Graaf, S.L. Njo, K.S. Smirnov, in: K.B. Lipkowitz, D.B. Boyd (Eds.), Reviews in Computational Chemistry, Vol. 14, Wiley/VCH, New York, 2000, p. 137 (Chapter 3).
[3] A. Vimont, F. Thibault-Starzyk, J.C. Lavalley, J. Phys. Chem. B 104 (2000) 286.
[4] E.M. Flaningen, H. Khatami, H.A. Szymanski, Adv. Chem. Ser. 101 (1971) 201.
[5] A.J.M. de Man, R.A. van Santen, Zeolites 12 (1992) 269.
[6] A.J.M. de Man, S. Ueda, M.J. Annen, M.E. Davis, R.A. van Santen, Zeolites 12 (1992) 789.
[7] P. Bornhauser, G. Calzaferri, J. Phys. Chem. 100 (1996) 2035.
[8] K.A. Iyer, S.J. Singer, J. Phys. Chem. 98 (1994) 12670.
[9] K.A. Iyer, S.J. Singer, J. Phys. Chem. 98 (1994) 12679.
[10] M. Sitarz, M. Handke, W. Mozgawa, Spectrochim. Acta 55 (1999) 2831.
[11] V.A. Ermoshin, K.S. Smirnov, D. Bougeard, Chem. Phys. 202 (1996) 53.
[12] K.S. Smirnov, D. Bougeard, J. Phys. Chem. 97 (1993) 9434.
[13] G. Schrimpf, M. Schlenkrich, J. Brickmann, P. Bopp, J. Phys. Chem. 96 (1992) 7404.
[14] J.A. Creighton, H.W. Deckman, J.M. Newsam, J. Phys. Chem. 98 (1994) 448.
[15] M. Bärtsch, P. Bornhauser, G. Calzaferri, R. Imhof, J. Phys. Chem. 98 (1994) 2817.
[16] G. Deo, A.M. Turek, I.E. Wachs, D.R.C. Huybrechts, P.A. Jacobs, Zeolites 13 (1993) 365, and references cited therein.
[17] A.J.M. de Man, J. Sauer, J. Phys. Chem. 100 (1996) 5025.
[18] K.S. Smirnov, B. van de Graaf, Microporous Mater. 7 (1996) 133.

[19] K.S. Smirnov, Unpublished results, 2000.

[20] V.A. Ermoshin, K.S. Smirnov, D. Bougeard, Chem. Phys. 209 (1996) 41.

[21] M.W. Schmidt, K.K. Baldridge, J.A. Boatz, S.T. Elbert, M.S. Gordon, J.H. Jensen, S. Koseki, N. Matsunaga, K.A. Nguyen, S.J. Su, T.L. Windus, M. Dupuis, J.A. Montgomery, General atomic and molecular electronic structure system (GAMESS), J. Comput. Chem. 14 (1993) 1347.

[22] J.-R. Hill, J. Sauer, J. Phys. Chem. 99 (1995) 9536.

[23] E.M. Flaningen, in: J.A. Rabo (Ed.), Zeolite Chemistry and Catalysis, ACS Monograph, Vol. 171, American Chemical Society, Washington, DC, 1976, p. 80 (Chapter 2).